

Unusual phase transition in 1D localization and its observability in optics

S. I. Bozhevolnyi⁽¹⁾, I. M. Suslov⁽²⁾

⁽¹⁾ Centre for Nano Optics, University of Southern Denmark, Campusvej 55,
DK-5230 Odense, Denmark

⁽²⁾ P.L.Kapitza Institute for Physical Problems, 119334 Moscow, Russia
E-mail: suslov@kapitza.ras.ru

Localization of electrons in 1D disordered systems is usually described in the random phase approximation, when distributions of phases φ and θ , entering the transfer matrix, are considered as uniform. In the general case, the random phase approximation is violated, and the evolution equations are written in terms of the Landauer resistance ρ and the combined phases $\psi = \theta - \varphi$ and $\chi = \theta + \varphi$. The distribution of the phase ψ is found to exhibit an unusual phase transition at the point \mathcal{E}_0 when changing the electron energy \mathcal{E} , which manifests itself in the appearance of the imaginary part of ψ . The distribution of resistance $P(\rho)$ has no singularity at the point \mathcal{E}_0 , and the transition seems unobservable in the framework of condensed matter physics. However, the theory of 1D localization is immediately applicable to the scattering of waves propagating in a single-mode optical waveguide. Modern optical methods open a way to measure phases ψ and χ . As a result, the indicated phase transition becomes observable.

1. Introduction

Localization of electrons in 1D disordered systems can be described by different methods [1]. The most efficient of them is based on the use of the transfer matrix T , relating the amplitudes of plane waves on the left ($Ae^{ikx} + Be^{-ikx}$) and on the right ($Ce^{ikx} + De^{-ikx}$) of a scatterer,

$$\begin{pmatrix} A \\ B \end{pmatrix} = T \begin{pmatrix} C \\ D \end{pmatrix}. \quad (1)$$

The matrix T can be parametrized in the form [2]

$$T = \begin{pmatrix} 1/t & -r/t \\ -r^*/t^* & 1/t^* \end{pmatrix} = \begin{pmatrix} \sqrt{\rho+1} e^{i\varphi} & \sqrt{\rho} e^{i\theta} \\ \sqrt{\rho} e^{-i\theta} & \sqrt{\rho+1} e^{-i\varphi} \end{pmatrix}, \quad (2)$$

if the presence of the time-reversal invariance is suggested; here t and r are the amplitudes of transmission and reflection, while $\rho = |r/t|^2$ is the dimensionless Landauer resistance [3]. If scatterers are arranged successively, their transfer matrices are multiplied. The transfer matrix T of a weak scatterer is close to the unit one, allowing to derive the differential evolution equations for its parameters.

Usually, such equations are derived in the random phase approximation, which is successfully used in the different areas of physics, though its limitations are also understood [4]–[10]. Its application in respect to the transfer matrix suggests the uniform distributions of φ and θ [11]–[16]. Such approximation

is sufficiently good for weak disorder well within the allowed band, as is widely accepted (see references in [1, 17, 18]). The fluctuation states in the forbidden band are considered infrequently [19, 20, 21] and only at the level of wave functions. A systematic analysis shows that the random phase approximation is strongly violated near the initial band edge and in the forbidden band of an ideal crystal [22]. In the general case, the evolution equations are written in terms of the Landauer resistance ρ and the combined phases (Sec.2)

$$\psi = \theta - \varphi, \quad \chi = \theta + \varphi. \quad (3)$$

The phase χ does not affect the evolution of ρ and is not interesting for the condensed matter physics. The distribution of the phase ψ was considered in the papers [23, 24] and undergoes the peculiar phase transition at the point \mathcal{E}_0 under the change of the electron energy \mathcal{E} [24] (Sec.3). Meanwhile, the distribution of resistance $P(\rho)$ has no singularity at the point \mathcal{E}_0 , and the transition looks unobservable in the framework of condensed matter physics.

However, the approach developed previously [22, 23, 24] is immediately applicable to the scattering of waves propagating in a single-mode optical waveguide (Sec.4). Existent optical methods (heterodyne approach, near-field microscopy, etc.) are rather efficient, and allows one to measure distributions of all

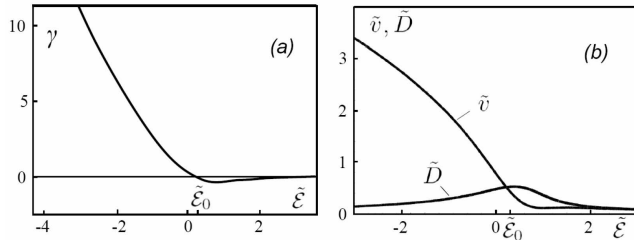


Figure 1: Dependence of parameters γ , $\tilde{v} = v/W^{2/3}$ and $\tilde{D} = D/W^{2/3}$ on the reduced energy $\tilde{\mathcal{E}} = \mathcal{E}/W^{4/3}$, obtained from the analysis of moments for the transfer matrix elements [22]. These moments are regular functions of energy, which leads to regularity of the presented dependencies. Smallness of γ and the equality $v = D$, valid in the random phase approximation, are realized only in the deep of the allowed band. The point $\tilde{\mathcal{E}}_0$ corresponds to the phase transition in the distribution $P(\psi)$.

parameters ρ , ψ , χ inside the waveguide¹ (Sec.6), and the indicated phase transition appears to be observable (Secs.5, 6). The general scheme of measurement suitable for this purpose is described in Sec.7.

2. Evolution equations

The most general evolution equation describes the change of the mutual distribution $P(\rho, \psi, \chi)$ under increasing of the system length L and has the following structure²

$$\frac{\partial P}{\partial L} = \left\{ \hat{L}_{\rho, \psi} P \right\}'_{\rho} + \left\{ \hat{M}_{\rho, \psi} P \right\}'_{\psi} + \left\{ \hat{K}_{\rho, \psi, \chi} P \right\}'_{\chi}, \quad (4)$$

where \hat{K} , \hat{L} , \hat{M} are operators, depending on indicated variables. The right-hand side is the sum of full derivatives, which ensures the conservation of probability. Integration of Eq.4 over χ allows to obtain the evolution equation for $P(\rho, \psi)$

$$\frac{\partial P}{\partial L} = \left\{ \hat{L}_{\rho, \psi} P \right\}'_{\rho} + \left\{ \hat{M}_{\rho, \psi} P \right\}'_{\psi}, \quad (5)$$

¹ In this context, the parameter ρ does not have a meaning of Landauer resistance, but determines the amplitudes of transmitted and reflected waves (Sec.5).

² Equation (4) was derived in the course of preparation of the papers [23, 24]; its complete form was not actual, and only its reduced variant (5) was published. Since the phase χ becomes observable (Sec.6), derivation of (4) and detailed analysis of the χ distribution will be a subject of future publications. Representation of the right-hand side as a sum of full derivatives is a common property of the Fokker-Planck equations, providing conservation of probability. The only specific feature of Eq.4 is independence on χ for operators \hat{L} and \hat{M} . This property can be deduced from the fact, that the evolution equation becomes closed on the level of two variables ρ and ψ .

whose specific form is given in [23, 24]. In the large L limit, the typical values of ρ are large, and the operator $\hat{M}_{\rho, \psi}$ becomes independent of ρ ; then the solution of Eq.5 is factorized, $P(\rho, \psi) = P(\rho)P(\psi)$, though a situation is somewhat unusual for separation of variables [24, 25]. The equation for $P(\psi)$ is split off, providing the existence of the stationary distribution of the phase ψ . The equation for $P(\rho)$ has a form

$$\frac{\partial P(\rho)}{\partial L} = D \frac{\partial}{\partial \rho} \left[-\gamma(1+2\rho)P(\rho) + \rho(1+\rho) \frac{\partial P(\rho)}{\partial \rho} \right], \quad (6)$$

and gives the log-normal distribution

$$P(\rho) = \frac{1}{\rho\sqrt{4\pi DL}} \exp \left\{ -\frac{[\ln \rho - vL]^2}{4DL} \right\}, \quad (7)$$

with $v = (2\gamma+1)D$. The typical value of ρ increases exponentially with L , which is an observable manifestation of 1D localization. In the random phase approximation, the parameter γ turns to zero, and equations (6), (7) coincide with the previously obtained results [11]–[16]. Dependencies of γ , D , v on the reduced energy $\tilde{\mathcal{E}} = \mathcal{E}/W^{4/3}$ are shown in Fig.1, where \mathcal{E} is the energy counted from the initial band edge, and W is an amplitude of the random potential; all energies are measured in units of the hopping integral of the 1D Anderson model, which is of the order of the initial band width. Strong violation of the random phase approximation is thereby evident (Fig.1).

3. Phase transition in the distribution $P(\psi)$

The meaning of the phase transition in the ψ distribution consists in the fact that difference between the allowed and forbidden bands survives (in a certain sense) in the presence of the random potential, though a singularity in the density of states is smoothed out. It resembles the famous argumentation by Mott [26], that the role of the allowed band edge comes to the mobility edge. Although the mobility edge is absent in the 1D case, a general situation appears to be analogous. The point is that the probe scatterer in the allowed band ($\mathcal{E} > 0$) is described by the transfer matrix (2), while in the forbidden band ($\mathcal{E} < 0$) it is described by the pseudo-transfer matrix \mathcal{T} [22], relating coefficients of the increasing and decreasing exponents on the left ($Ae^{\kappa x} + Be^{-\kappa x}$) and on the right ($Ce^{\kappa x} + De^{-\kappa x}$) of the scatterer. In the simplest case, the matrix \mathcal{T} is real and corresponds

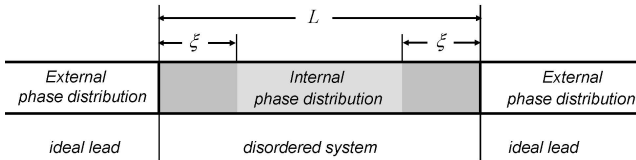


Figure 2: External and internal phase distributions.

to pure imaginary values of phases θ and φ . Let us compare situations for $\mathcal{E} > 0$ and $\mathcal{E} < 0$: for a sufficient separation in energy, the difference between two types of matrices can be made arbitrary large, and it cannot be overcome by inclusion of a weak random potential. As a result, the border-line between the true and pseudo transfer matrices can only be shifted, but not eliminated. In practice, it is manifested via the appearance of the imaginary part of the phase ψ for energies $\mathcal{E} < \mathcal{E}_0$ [24].

The formal statements of the paper [24] reduce to the following. First of all, one should differ the 'external' and 'internal' phase distributions (Fig.2). The internal phase distribution is realized in the deep of a sufficiently long disordered system, and is independent of boundary conditions. The phases entering the transfer matrix refer to the 'external' phase distribution, which depends on the boundary conditions and can be observed from the side of the ideal leads. The internal phase distribution continually transforms to the external one in the transient region of the order of the localization length ξ , where influence of interfaces is essential. Independence of the limiting distribution $P(\rho)$ (Eq.7) from the boundary conditions is evident from this picture, since it is determined by the internal phase distribution. However, the evolution equations contain not internal, but the external phase distribution, and one wonders why it does not affect the limiting distribution $P(\rho)$. There is the second question, related with the first one, and it can be formulated as follows: how the internal phase distribution can be found, if it does not appear in the evolution equations?

The above questions are resolved in the following manner. It appears, that the phase ψ is a 'bad' variable, while the 'correct' variable should be defined as

$$w = -\cot \psi/2. \quad (8)$$

The form of the stationary distribution $P(w)$ is independent of boundary conditions, being determined by only internal properties of the system. If the bound-

ary conditions are changed, it leads to three effects: the scale transformation $w \rightarrow sw$ and two translations $w \rightarrow w + w_0$ and $\psi \rightarrow \psi + \psi_0$. The corresponding changes of the distribution $P(\psi)$ are easily predictable [24] and can be observed in the external phase distribution. The evolution equations are invariant in respect to translation $\psi \rightarrow \psi + \psi_0$, and the internal phase distribution can be discussed under the fixed choice of the origin. Invariance of the limiting distribution $P(\rho)$ under transformations $w \rightarrow sw$ and $w \rightarrow w + w_0$ is realized in the dynamical manner. Analogously to aperiodic oscillations of $P(\rho)$ [22, 27, 28], in the region $L \lesssim \xi$ the scale factor s and the translational shift w_0 undergo aperiodic oscillations as functions of L , attenuating at large L . As a result, s and w_0 tend to the certain 'correct' values, which provide the correct values of D and v in the limiting distribution (7). The indicated 'correct' values correspond to the internal phase distribution, and the latter can be found after return to the variable ψ . Meanwhile, it appears that the translational shift w_0 becomes complex-valued for $\mathcal{E} < \mathcal{E}_0$, indicating the occurrence of the imaginary part of ψ . This qualitative change indicates existence of the unusual phase transition.

The point \mathcal{E}_0 is not singular for the Landauer resistance ρ , and the whole distribution $P(\rho)$ varies in its vicinity in a smooth manner (Fig.1,b). As a result, the described phase transition looks unobservable in the framework of the condensed matter physics. Fortunately, it has the observable manifestations in optics (Secs.5,6) in the form of the square root singularities.

4. Analogy with optics

Localization of classical waves was discussed in a number of papers [29]–[35], [17, 18]. It includes consideration of weak [30] and strong [31, 32] localization, absorption near a photon mobility edge [29], near-field mapping of intensity of optical modes in disordered waveguides [33], and many other aspects (see the review article [34]. The transfer matrix approach to the problem was discussed in [17, 18, 35]. In application to optics the corresponding analysis reduces to a set of simple relations.

Propagation of electromagnetic waves in homogeneous dielectric media is described by the wave equation

$$c^2 \Delta \Psi - n^2 \frac{\partial^2 \Psi}{\partial t^2} = 0, \quad (9)$$

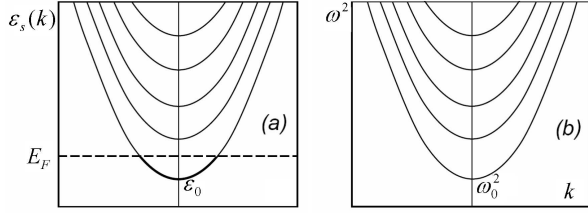


Figure 3: The spectrum of electrons in the metallic wire (a), and the spectrum of waves propagating in a waveguide (b).

where Ψ is any component of the electric or magnetic field. If a medium is spatially inhomogeneous, the refractive index n is varying along the coordinate x ,

$$n^2(x) = n_0^2 + \delta n^2(x), \quad (10)$$

and for the monochromatic wave $\Psi \sim e^{i\omega t}$, the wave equation can be written in the form

$$\tilde{c}^2 \Delta \Psi + \left[\omega^2 + \omega^2 \frac{\delta n^2(x)}{n_0^2} \right] \Psi = 0, \quad \tilde{c} = c/n_0. \quad (11)$$

The latter exhibits the same structure, as the Schrödinger equation for an electron with energy \mathcal{E} and mass m in the random potential $V(x)$. One can easily establish the correspondence

$$\mathcal{E} \iff \omega^2, \quad \frac{1}{2m} \iff \tilde{c}^2, \quad V(x) \iff -\omega^2 \frac{\delta n^2(x)}{n_0^2}. \quad (12)$$

A certain difference from the condensed matter physics is related to the ω dependence of the potential $V(x)$, which of little importance, if one is restricted by a small frequency interval of the continuous spectrum.

The spectrum of waves propagating in a waveguide is analogous to the spectrum of electrons in a metallic wire. In the latter case, the transverse motion is quantized, leading to a set of the discrete levels ϵ_s . If the longitudinal motion is taken into account, these levels transform to one-dimensional bands with the dispersion law (Fig.3,a)

$$\epsilon_s(k) = \epsilon_s + k^2/2m. \quad (13)$$

To obtain a strictly 1D system, one should have a sufficiently small Fermi level so that only the lowest band is occupied. In the presence of impurities, the lower boundary ϵ_0 of the spectrum is smeared out due to the occurrence of fluctuation states for $\mathcal{E} < \epsilon_0$.

The dependencies shown in Fig.1 correspond to the energy \mathcal{E} counted from ϵ_0 .

Analogously, quantization of the transverse motion in a waveguide leads to a set of discrete frequencies $\omega_s = \tilde{c}\kappa_s$, where $-\kappa_s^2$ are eigenvalues of the 2D Laplace operator with the appropriate boundary conditions [36]. The zero eigenvalue is possible only in the case, when the waveguide cross-section is multiply connected (e.g. as in a coaxial cable). For a singly connected cross-section, the minimum eigenvalue ω_0 is finite [36]. If the longitudinal motion is taken into account, the following branches of the spectrum are obtained (Fig.3,b)³

$$\omega_s^2(k) = \omega_s^2 + \tilde{c}^2 k^2. \quad (14)$$

To realize a single-mode waveguide regime, one should operate near the lower boundary ω_0 of the spectrum. In the presence of disorder, the spectrum boundary ω_0 is smeared out due to the occurrence of the fluctuation states. Overall, the effects appearing in the electron system under the change of the Fermi level can be observed in a single-mode waveguide under the change of frequency ω in the vicinity of ω_0 .

5. Detection of the phase transition

Let a wave of the unit amplitude be incident from the left side of a single-mode waveguide, and comes through it with the amplitude t , being reflected with the amplitude r . If there are point scatterers in the waveguide, then a partial reflection occurs at any of them. Thus, at an arbitrary point x of the waveguide one finds a superposition of two waves, propagating in opposite directions. The electric field $E(x, t)$ is determined by the real part of this superposition, i.e.

$$E(x, t) = \text{Re} [Ae^{ikx+i\omega t} + Be^{-ikx+i\omega t}]. \quad (15)$$

With the transfer matrix T being defined by Eqs.(1,2), the amplitudes of the transmitted and reflected waves are determined by the expression

$$\begin{pmatrix} A \\ B \end{pmatrix} = T \begin{pmatrix} t \\ 0 \end{pmatrix} = \begin{pmatrix} |t|\sqrt{\rho+1} e^{i\varphi-i\varphi_0} \\ |t|\sqrt{\rho} e^{-i\theta-i\varphi_0} \end{pmatrix}, \quad (16)$$

³ We have in mind a metal-coated dielectric waveguide. The coating thickness should be of the order of the skin depth in order to allow for partial field penetration outside the waveguide (see Sec.7). In the absence of coating (a pure dielectric waveguide), one should take into account the frequency dependence of the effective potential $V(x)$ (see Eq.11), which leads to lower restrictions for the allowed values of the longitudinal momenta k (conditions for the total internal reflection are violated). In addition, the parameters κ_s cease to be constant and become ω -dependent, resulting in deviations from the parabolic dependencies in Fig.3,b.

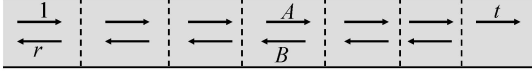


Figure 4: Propagation of waves in the single-mode waveguide with point scatterers.

where ρ , φ , θ are x -dependent and $t = |t|e^{-i\varphi_0}$ is adopted. If the amplitude $|t|$ is sufficiently small, then the quantity ρ is large in the whole waveguide, except the vicinity of its right end. Then $|A| \approx |B|$, and Eq.15 gives in this approximation

$$E(x, t) = \text{Re} \left[|A| e^{ikx+i\varphi-i\varphi_0} + |B| e^{-ikx-i\theta-i\varphi_0} \right] e^{i\omega t} \\ \approx 2|A| \cos(kx + \chi/2) \cos(\omega t - \psi/2 - \varphi_0), \quad (17)$$

where the combined phases ψ and χ are defined in Eq.3: they remain constant between the scatterers, and change abruptly when passing through a scatterer. If the concentration of impurities is large, then ψ and χ change with x practically continuously, having random variations on the scale of the scattering length.

Since the field $E(x, t)$ can be measured in principle, both phases χ and ψ are theoretically observable. This is the fundamental difference from the condensed matter physics, where a superposition of waves refers to a wave function, and should be squared in modulus to obtain the observable quantities: in this case the phase ψ is unobservable in principle. This phase would become unobservable in optics, if only the average intensity could be measured (it means that equation (17) is squared and averaged over time). It is easy to verify, that this conclusion remains valid also for $|A| \neq |B|$.

Nevertheless, the occurrence of the imaginary part of ψ can be registered even in this case. If we suppose that

$$\varphi = \varphi' + i\varphi'', \quad \theta = \theta' + i\theta'', \quad (18)$$

then the amplitudes in the linear combination (15) accept the form

$$|A| = |t|\sqrt{\rho+1}e^{-\varphi''}, \quad |B| = |t|\sqrt{\rho}e^{\theta''}. \quad (19)$$

The flux conservation requires⁴ that the condition $|A|^2 = |B|^2 + |t|^2$ be fulfilled at the arbitrary point of

⁴ A scattering is considered as pure elastic. Inevitable Ohmic losses in the metal coating (see Footnote 2) are suggested to be essentially weaker in comparison with localization effects.

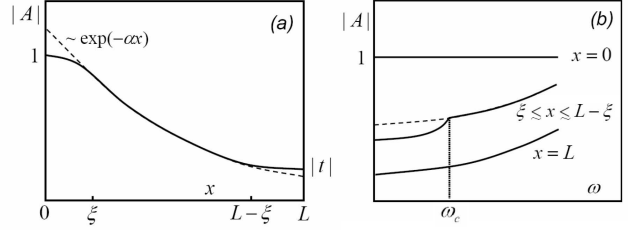


Figure 5: (a) Dependence of the amplitude $|A|$ of the transmitted wave on the coordinate x inside the waveguide. (b) The amplitude $|A|$ versus a frequency ω in the vicinity of the phase transition.

the waveguide, which leads to relation

$$(\rho+1)e^{-\varphi''} = \rho e^{\theta''} + 1 \quad (20)$$

giving $\theta'' = -\varphi''$ for large ρ . The imaginary part is absent in the phase χ , but is admissible for the phase ψ ; in the latter case $\psi'' = 2\theta'' = -2\varphi''$, and in particular

$$|A| = |t|\sqrt{\rho+1}e^{\psi''/2}. \quad (21)$$

According to [24], the imaginary part of ψ appears as a result of solution of certain equations, and its behavior can be established from the general considerations. Let we have the equation $F(x) = 0$, where the function $F(x)$ depends regularly on the external parameter ϵ . If at the point $\epsilon = 0$ two real roots become complex-valued, then the multiple root $x = p$ takes place for $\epsilon = 0$, and in its vicinity one has the equation

$$(x - p)^2 - \epsilon = 0, \quad (22)$$

which gives roots $p \pm \sqrt{\epsilon}$ for $\epsilon > 0$ and roots $p \pm i\sqrt{|\epsilon|}$ for $\epsilon < 0$. Thereby, the appearance of the imaginary part is related with a square root singularity. If the imaginary part of ψ appears for $\omega < \omega_c$, then it has a behavior

$$\psi'' \sim \sqrt{\omega_c - \omega} \Theta(\omega_c - \omega). \quad (23)$$

According to [24], the distribution $P(\rho)$ is not singular at the point ω_c (Fig.1,b). It refers to a value of ρ at the arbitrary point of the waveguide, and in particular to its value at the whole length L , which is related with t as $|t| = (1 + \rho)^{-1/2}$. Therefore, the singularity in the amplitude (21) is completely determined by the quantity ψ'' and has a square root character.

The general picture looks as follows (Fig.5). In whole, the modulus of A changes in the waveguide

according to the exponential law, $|A| \sim e^{-\alpha x}$, but deviations from it arise on the scale ξ near the ends due to influence of boundary conditions (Fig.5,a): in particular, $|A| = 1$ for $x = 0$ and $|A| = |t|$ for $x = L$. The latter quantity is related with ρ and is a regular function of ω . However, in the deep of the waveguide the amplitude $|A|$ has a square root singularity (Fig.5,b), which can be registered already in the measurements of the average intensity.

According to [24], the critical point \mathcal{E}_0 is situated in the allowed band at the distance of order $W^{4/3}$ from the band edge. Correspondingly, in optics the critical point ω_c is greater than the boundary frequency ω_0 , while a distance between them is determined by the degree of disorder.

6. Observability of phases ψ and χ

Measurements of the time dependence at optical frequencies are usually impossible. However, observability of the phase ψ can be provided with heterodyne technique, in which the measured electric field $E(x,t)$ is mixed with the additional field $E_s(x,t)$, whose frequency is shifted by a small quantity Ω :

$$E + E_s = \text{Re} \left\{ |E|e^{i\omega t + i\varphi_E} + |E_s|e^{i(\omega + \Omega)t + i\varphi_s} \right\}. \quad (24)$$

Considering the intensity averaged over fast time oscillations, one has

$$2\overline{(E + E_s)^2} = |E|^2 + |E_s|^2 + 2|E||E_s| \cos(\Omega t + \varphi_s - \varphi_E). \quad (25)$$

Substituting $E(x,t)$, corresponding to expression (17), one obtains

$$\begin{aligned} 2\overline{(E + E_s)^2} = & \{4|A|^2 \cos^2(kx + \chi/2) + |E_s|^2\} + \\ & + 2|A| \cos(kx + \chi/2) \cdot 2|E_s| \cos(\Omega t + \psi/2 + \varphi_0 + \varphi_s). \end{aligned} \quad (26)$$

so both phases χ and ψ are observable, and can be extracted from the experiment by the following treatment.

The stationary first term and the oscillatory second term in Eq.(26) can be separated by the Fourier filtering in the time domain. The constant term $|E_s|^2$ can then be easily extracted, since the smallest value of the first term in the braces is zero. Since the cosine changes regularly and reverses sign at any zero, the square root from the first term in braces can be extracted to inessential common sign. As a result, two combinations would separately become known

$$|A| \cos(kx + \chi/2) \quad \text{and} \quad |E_s| \cos(\Omega t + \psi/2 + \varphi_0 + \varphi_s) \quad (27)$$

The factor $|E_s|$ in the second combination is determined by the amplitude of its temporal oscillations⁵, while its x dependence can be attributed to the spatial dependence of the phase ψ .

The treatment of the first combination (27) is complicated by the fact that the amplitude $|A(x)|$ does not follow strictly the exponential dependence $\exp(-\alpha x)$, but exhibits significant fluctuations around it according to the log-normal distribution (7). The appropriate treatment looks as follows:

1. Find a value of k by evaluating the average spatial period of oscillations.

2. Find values of χ at the sequence of discrete points, which are maxima, minima and zeroes of the oscillating dependence, by assessing deviations of their position from those of the purely cosine function. If the value of k is estimated correctly, then the obtained χ values would fluctuate around a constant value and not exhibit a systematic growth. As a result, one obtains a sufficient material for the analysis of the χ distribution.

3. Find values of $|A(x)|$ at the points of maxima and minima. These values would provide sufficient data for verifying the log-normal distribution, and allow to reveal systematic deviations from the exponential dependence near the waveguide ends.

Observability of the phase ψ provides additional possibilities for registration of the phase transition. If one introduce the variable w defined in Eq.(8), then the moments of the distribution $P(w)$ (e. g. $\langle w \rangle$) will have the singularities $\sqrt{\omega - \omega_c}$ in the region $\omega > \omega_c$. The phase χ does not affect the evolution of $P(\rho)$ and was not studied in the papers [23, 24]. However, the possibility of its observation in optics makes such studies to be actual.

7. The general measurement scheme

The electrical field in a waveguide can be measured using methods of the scanning near-field optical microscopy [37, 38, 39]. In the scheme considered below, a near-field microscope probe (which is usually a fragment of an optical fiber with a pointed tip) is used not for the immediate field detection, but only as a source of scattering⁶ with subsequent use of a remote

⁵ Another way to reach the same result is to make measurements for several values of $|E_s|$ and fit the right-hand side of (26) by the dependence $\alpha + \beta|E_s| + \gamma|E_s|^2$.

⁶ It can be replaced by a needle of a scanning tunneling microscope, which in the presence of metal coating (see Footnote 2) allows one to use all advantages of the scanning tunneling electron microscopy.

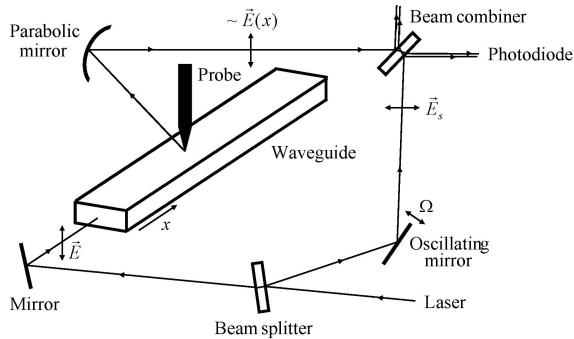


Figure 6: Measurement of the electric field in the waveguide using the scanning near-field optical microscope.

detector. A wave propagating in the waveguide penetrates beyond its boundaries due to the tunneling effect and can be scattered by a probe tip located close to a waveguide surface. For subwavelength-sized probe tips, the scattering occurs in the Rayleigh regime with the field of the scattered wave being proportional to the local electric field $E(x, t)$ at the point of scattering x .⁷

The general scheme of field measurement looks as follows (Fig.6). A laser beam is split into two parts, one of which is directed into a waveguide and eventually scattered by a microscope probe tip. The scattered light is collected by a parabolic mirror and directed to a beam combiner. The second part of the laser beam is reflected by an oscillating mirror, acquiring a small frequency shift Ω due to the Doppler effect. Since the mirror velocity is variable, it leads to a variable shift Ω . This problem can however be solved, if the time dependence is registered at the discrete points, equally spaced by the period of mirror oscillations. Another possibility consists in realization of the saw-toothed regime of oscillations instead of the harmonic one. After the mirror, the beam is directed to the beam combiner, where it is mixed with the first beam and follows to a photodiode for measurement of intensity.

The described scheme was realized in studies reported in the paper [40], where additional experimental details can be found. In contrast to the

⁷ In the Rayleigh scattering, the electromagnetic field of the scattered wave is determined (in the main approximation) by the electric field of the incident wave and does not depend on the wave vector of the latter [36]. As a result, two waves entering the superposition (15) are scattered equally, and the total field of the scattered wave appears to be proportional to the electric field in the waveguide.

papers [41, 42], where only the transmission matrix was measured, Ref.[40] presents the experimental approach allowing to measure the phase distribution inside the waveguide. Ref.[40] deals with surface plasmon polaritons, i.e. electromagnetic excitations, propagating along a metal-dielectric interface. In the transverse direction they are localized on the scale about 100nm, which is an order of magnitude less than a typical size of a single-mode waveguide. The latter is not essential, since their transverse profile extends to the air side in the same manner, as for waves propagating in a waveguide and tunneling through its boundaries. Correspondingly, they are subjected to analogous scattering by the microscope probe. The spectrum of surface waves is analogous the that of the metallic waveguide (Fig.3,b), and the single-mode regime was realized in Ref.[40]. However, the measurements of Ref.[40] were not concerned with light propagation in disordered systems, but only with characterization of regular modes in homogeneous waveguides.

Essentially new measurements are necessary for testing the validity of claims made in the present paper. These experiments should overcome certain experimental difficulties. Firstly, the most promising waveguide configuration should be established, along with the approach for introducing properly disordered defects into the waveguide. Extensive analysis is necessary to find the parameter range, where the localization effects will be dominating over the light absorption inside the waveguide and radiative losses through its boundaries. Finally, the actual experiments should be executed using a tunable laser allowing to change the light frequency, and its tunability range should cover the targeted phase transition. This is a very ambitious and demanding project going far beyond the framework of the current work.

8. Conclusion

It has been shown that all results obtained for electrons in 1D disordered systems are immediately applicable to the propagation of electromagnetic waves in single-mode optical waveguides. It has also been argued that modern optical techniques, such as near-field microscopy, enable measurements of all parameters entering the transfer matrix. In particular, it becomes possible to observe the phase transition for the distribution $P(\psi)$, which seems unobservable in the framework of the condensed matter physics. We believe that the results obtained might stimulate the corresponding experimental activities that would, in

turn, shed more light on intricate effects in both optical and electron localization phenomena.

References

- [1] I. M. Lifshitz, S. A. Gredeskul, L. A. Pastur, Introduction to the Theory of Disordered Systems, Nauka, Moscow, 1982.
- [2] P. W. Anderson, D. J. Thouless, E. Abrahams, D. S. Fisher, Phys. Rev. B **22**, 3519 (1980).
- [3] R. Landauer, IBM J. Res. Dev. **1**, 223 (1957); Phil. Mag. **21**, 863 (1970).
- [4] X. Ren, A. Tkatchenko, P. Rinke, M. Scheffler, Phys. Rev. Lett. **106**, 153003 (2011).
- [5] X. Ren, P. Rinke, Ch. Joas, M. Scheffler, J. Mater. Sci. **47**, 7447 (2012).
- [6] T. Olsen, K. S. Thygesen, Phys. Rev. B **88**, 115131 (2013).
- [7] J. Klime, M. Kaltak, E. Maggio, G. Kresse, J. Chem. Phys. **143**, 102816 (2015).
- [8] T. Gould, J. Toulouse, J. G. Angyan, J. F. Dobson, J. Chem. Theory Comput. **13**, 5829 (2017).
- [9] M. Panholzer, R. Hobbiger, H. Bohm, Phys. Rev. B **99**, 195156 (2019).
- [10] T. Gould, A. Ruzsinszky, J. P. Perdew Phys. Rev. A **100**, 022515 (2019).
- [11] V. I. Melnikov, Sov. Phys. Sol. St. **23**, 444 (1981).
- [12] A. A. Abrikosov, Sol. St. Comm. **37**, 997 (1981).
- [13] N. Kumar, Phys. Rev. B **31**, 5513 (1985).
- [14] B. Shapiro, Phys. Rev. B **34**, 4394 (1986).
- [15] P. Mello, Phys. Rev. B **35**, 1082 (1987).
- [16] B. Shapiro, Phil. Mag. **56**, 1031 (1987).
- [17] C. W. J. Beenakker, Rev. Mod. Phys. **69**, 731 (1997).
- [18] X. Chang, X. Ma, M. Yezpez, A. Z. Genack, P. A. Mello, Phys. Rev. B **96**, 180203 (2017).
- [19] L. I. Deych, D. Zaslavsky, A. A. Lisyansky, Phys. Rev. Lett. **81**, 5390 (1998).
- [20] L. I. Deych, A. A. Lisyansky, B. L. Altshuler, Phys. Rev. Lett. **84**, 2678 (2000); Phys. Rev. B **64**, 224202 (2001).
- [21] L. I. Deych, M. V. Erementchouk, A. A. Lisyansky, Phys. Rev. Lett. **90**, 126601 (2001).
- [22] I. M. Suslov, J. Exp. Theor. Phys. **129**, 877 (2019) [Zh. Eksp. Teor. Fiz. **156**, 950 (2019)].
- [23] I. M. Suslov, Phil. Mag. Lett. **102**, 255 (2022).
- [24] I. M. Suslov, J. Exp. Theor. Phys. **135**, 726 (2022) [Zh. Eksp. Teor. Fiz. **162**, 750 (2022)].
- [25] I. M. Suslov, Adv. Theor. Comp. Phys. **6**, 77 (2023).
- [26] N. F. Mott, E. A. Davis, Electron Processes in Non-Crystalline Materials, Oxford, Clarendon Press, 1979.
- [27] V. V. Brazhkin, I. M. Suslov, J. Phys. – Cond. Matt. **32** (35), 35LT02 (2020).
- [28] I. M. Suslov, J. Exp. Theor. Phys. **131**, 793 (2020) [Zh. Eksp. Teor. Fiz. **158**, 911 (2020)].
- [29] S. John, Phys. Rev. Lett. **53**, 2169 (1984).
- [30] P. Van Albada, A. Lagendijk, Phys. Rev. Lett. **55**, 2692 (1985).
- [31] P. W. Anderson, Philos. Mag. B **52**, 505 (1985).
- [32] S. John, Phys. Rev. Lett. **58**, 2486 (1987).
- [33] S. I. Bozhevolnyi, V. S. Volkov, K. Leosson, Phys. Rev. Lett. **89**, 186801 (2002).
- [34] D. S. Wiersma, Nature Photon. **7**, 188 (2013).
- [35] Zh. Shi, M. Davy, A. Z. Genack, Opt. Express **23**, 12293 (2015).
- [36] L. D. Landau, E. M. Lifshits, Electrodynamics of Continuous Media, Oxford, Pergamon Press, 1984.
- [37] D. W. Pohl, W. Denk, M. Lanz, Appl. Phys. Lett. **44**, 651 (1984).
- [38] D. W. Pohl, L. Novotny, J. Vac. Sci. Technol. B **12**, 1441 (1994).
- [39] A. L. Leren, A. Passian, Ph. Dumas, Int. J. Nanotechnol. **9**, 488 (2012).

- [40] V. A. Zenin, R. Malreanu, I. P. Radko, A. V. Lavrinenko, S. I. Bozhevolnyi, *Opt. Express* 24, 4582 (2016).
- [41] I. M. Vellekoop and A. P. Mosk, *Phys. Rev. Lett.* 101, 120601 (2008).
- [42] S. M. Popoff, G. Lerosey, R. Carminati, M. Fink, A. C. Boccara, and S. Gigan, *Phys. Rev. Lett.* 104, 100601 (2010).